Published in final edited form as:
Nature. 2012 May 3; 485(7396): 99–103. doi:10.1038/nature10997.

Restoration of vision after transplantation of photoreceptors

R. A. Pearson[1], **A. C. Barber**[1], **M. Rizzi**[1], **C. Hippert**[1], **T. Xue**[3], **E. L. West**[1], **Y. Duran**[1], **A. J. Smith**[1], **J. Z. Chuang**[4], **S. A. Azam**[1], **U. F. O. Luhmann**[1], **A. Benucci**[2], **C. H. Sung**[4], **J. W. Bainbridge**[1], **M. Carandini**[2], **K.-W. Yau**[3], **J. C. Sowden**[5], and **R. R. Ali**[1,6]

[1]Department of Genetics UCL Institute of Ophthalmology, University College London, 11–43 Bath Street, London, EC1V 9EL, UK

[2]Department of Visual Neuroscience, UCL Institute of Ophthalmology, University College London, 11–43 Bath Street, London, EC1V 9EL, UK

[3]Solomon H. Snyder Department of Neuroscience, The Johns Hopkins University School of Medicine, Baltimore, Maryland 21205, USA

[4]Dyson Vision Research Institute, Department of Ophthalmology, Department of Cell and Developmental Biology, Weill Medical College of Cornell University, New York, New York 10021, USA

[5]Developmental Biology Unit, UCL Institute of Child Health, University College London, 30 Guilford Street, London, WC1N 1EH, UK

[6]Molecular Immunology Unit, UCL Institute of Child Health, University College London, 30 Guilford Street, London, WC1N 1EH, UK

Cell transplantation is a potential strategy for treating blindness caused by the loss of photoreceptors. Although transplanted rod-precursor cells are able to migrate into the adult retina and differentiate to acquire the specialized morphological features of mature photoreceptor cells[1], the fundamental question remains whether transplantation of photoreceptor cells can actually improve vision. Here we provide evidence of functional rod-mediated vision after photoreceptor transplantation in adult *Gnat1*$^{-/-}$ mice, which lack rod function and are a model of congenital stationary night blindness[2]. We show that transplanted rod precursors form classic triad synaptic connections with second-order bipolar and horizontal cells in the recipient retina. The newly integrated photoreceptor cells are light-responsive with dim-flash kinetics similar to adult wild-type photoreceptors. By using intrinsic imaging under scotopic conditions we demonstrate that visual signals generated by transplanted rods are projected to higher visual areas, including V1. Moreover, these cells are capable of driving optokinetic head tracking and visually guided behaviour in the *Gnat1*$^{-/-}$ mouse under scotopic conditions. Together, these results demonstrate the

Correspondence and requests for materials should be addressed to R.A.P. (rachael.pearson@ucl.ac.uk) or R.R.A. (r.ali@ucl.ac.uk).

Supplementary Information is linked to the online version of the paper at www.nature.com/nature.

Author Contributions R.A.P. contributed to the concept, design, execution and analysis of all experiments, funding, and wrote the manuscript. A.C.B. contributed to the design, execution and analysis of experiments except single-cell recordings, electron microscopy and behavioural assessments. M.R., A.B. and M.C. contributed to the design, execution and analysis of the intrinsic optical-imaging experiments. C.H., A.J.S. and S.A.A. contributed to the design and execution of the AAV gene supplementation studies, and C.H. the execution of the water-maze tests. Y.D. contributed to the histological processing and execution of the water-maze tests. J.W.B., E.L.W. and U.F.O.L. contributed to the optimization of transplantation protocols. T.X. performed the single-cell recordings. K.W.Y. contributed to the design and analysis of the single-cell recordings. C.H.S. and J.Z.C. performed the ultrastructural analysis. J.C.S. and R.R.A. contributed to the concept and design of the experiments, funding and to manuscript writing.

The authors declare no competing financial interests.

feasibility of photoreceptor transplantation as a therapeutic strategy for restoring vision after retinal degeneration.

So far there have been no convincing reports of photoreceptor-cell transplantation actually improving the recipient's vision. This may be due to the relatively low numbers of new rod photoreceptors successfully transplanted in previous studies (typically fewer than 1,000 cells)[1,3–6]. To establish that new rods truly can improve vision, we optimized the rod-transplantation procedure to increase the number of newly integrated photoreceptor cells in wild-type mice. The donor-cell population was rod-photoreceptor precursors identified by their expression of green fluorescent protein (GFP) under control of the promoter for the rod-specific transcription factor, *Nrl*[7]. We obtained maximum integration together with optimal recipient retinal histology after the transplantation of 200,000 fluorescence-activated cell sorted *Nrl-GFP*$^{+}$ rod precursors, taken from postnatal day (P) 4–8 *Nrl-GFP* donor mice, by subretinal injection to both the superior and the inferior retina. This resulted in a 20- to 30-fold increase in the number of integrated rod photoreceptors compared with previous studies, with up to 26,000 new rods within the outer nuclear layer of recipient adult wild-type mice (16,759 ± 1,705 cells; Fig. 1a and Supplementary Fig. 1). Integrated cells were found predominantly around the injection sites, but were distributed over more than 50%of the retinal area. Thus, up to 16% of donor cells integrated into the host outer nuclear layer (see Supplementary Information for estimation of integrated cell number). Supplementary Fig. 1 summarizes how this was achieved.

To test the functionality of the transplanted rod photoreceptors, we selected a murine model in which improvement of rod vision could be assessed definitively; the *Gnat1*$^{-/-}$ mouse lacks rod α-transducin (Gnat1), a protein essential for rod phototransduction. It has no rod function[2] or behavioural responses to scotopic visual stimuli; it displays, however, near-normal cone histology[8], function and behavioural responses to photopic visual stimuli (Supplementary Fig. 2 and refs 2, 9) and shows no loss of cones with time[8]. *Nrl-GFP*$^{+}$ rod precursors integrated into the adult *Gnat1*$^{-/-}$ retina in numbers very similar to those observed in wild-type recipients (18,300 ± 1474; maximum 32,015 integrated cells; Fig. 1a). Integrated cells were appropriately located within the outer nuclear layer and morphologically very similar to wild-type rods (Fig. 1b–i and Supplementary Fig. 3), correctly expressing rod α-transducin (Fig. 1c, d), which is absent in endogenous *Gnat1*$^{-/-}$ rods, together with all other mature rod markers examined (rod arrestin (Fig. 1e, f), rhodopsin, recoverin, phosducin (data not shown)). They demonstrated outer segment formation (Fig. 1b–f) and appropriate light-dependent translocation of rod α-transducin (Fig. 1c, d) and arrestin (Fig. 1e, f)[10] between the outer segments and the cell body/synapse. Most (>80%) of *Nrl-GFP*$^{+}$ rods located within the outer nuclear layer displayed synaptic boutons. All those examined by immunohistochemistry (15–20 cells per marker) appropriately expressed the rod ribbon synapse proteins ribeye, bassoon and/or dystrophin[11] (Fig. 1g–i). Finally, ultrastructural analysis confirmed that integrated *Nrl-GFP*$^{+}$ rods typically formed the classic triad synapse with endogenous horizontal and bipolar neurons (Fig. 1j, k; synapses observed for 51/55 cells examined; see Supplementary Information).

To test for light responses in *Nrl-GFP*$^{+}$ rods correctly integrated within *Gnat1*$^{-/-}$ recipients, we performed suction-pipette recordings[12] (Fig. 2a, b). Pigment bleached by the GFP-excitation light used during *Nrl-GFP*$^{+}$ cell searching was regenerated with 9-*cis*-retinal before recording (see Supplementary Information). To control for the effects of the bleaching/regeneration procedure on the speed of the dim-flash response kinetics and the sensitivity of wild-type rods (Fig. 2b,), we also recorded from non-injected wild-type retinae with and without the excitation-light/pigment-regeneration procedure (Fig. 2a, b). All recorded *Nrl-GFP*$^{+}$ rods with an intact inner segment, cell body and synaptic terminal showed light responses (n = 9/9; Fig. 2a, b). Their saturated photocurrent (4.6 ± 0.5 pA) was

similar to that of wild-type rods with or without bleaching/regeneration treatment (Fig. 2b; 6.4 ± 0.7 and 6.1 ± 0.8 pA, respectively). Dim-flash response kinetics, indicated by time-to-peak (t_{peak}) and integration time (t_i), were similar between *Nrl-GFP*$^+$ and wild-type rods subjected to bleaching/regeneration (see Fig. 2b). Individual *Nrl-GFP*$^+$ rods showed variations in sensitivity, with one cell being as sensitive as bleached/regenerated wild-type rods and the other three over a log unit less sensitive (Fig. 2b). This variation may be real, or simply reflect the small sample size (owing to technical challenges in obtaining this parameter in bleached/regenerated *Nrl-GFP*$^+$ rods). For each *Nrl-GFP*$^+$ rod recorded, several adjacent GFP^{-ve} rods were also tested; none gave detectable responses (Fig. 2c), thus ruling out light signals originating from cones in the *Gnat1*$^{-/-}$ retina.

Electroretinography (ERG) provides a gross measure of light-mediated trans-retinal function, averaged across the whole retina. *Gnat1*$^{-/-}$ mice received dual transplants of *Nrl-GFP*$^+$ rod precursors into one eye and equivalent sham injections (age-matched *Gnat1*$^{-/-}$ cells or vehicle) or no injection into the contralateral eye (Supplementary Fig. 4). ERGs were recorded weekly 3–6 weeks after transplantation using a double-masked protocol (see Supplementary Information), before the eyes were assessed for *Nrl-GFP*$^+$ rod-photoreceptor integration. Despite robust integration (7,135–26,616 integrated cells per eye; $n = 6$), ERG responses were not detected upon scotopic stimulation of procedured *Gnat1*$^{-/-}$ animals (Supplementary Fig. 4a). In contrast, such responses were readily recordable in wild-type animals (Supplementary Fig. 4f). These results were not unexpected because control experiments with an adeno-associated (AAV2/8) viral vector to deliver a *Gnat1* transgene showed that a scotopic ERG response was recordable only after transduction of approximately 150,000 photoreceptor cells, but not of 60,000 rods (Supplementary Fig. 4d–g). Robust responses were observed in all groups after photopic stimulation with no significant differences between sham and *Nrl-GFP*$^+$-treated eyes (Supplementary Fig. 4h). Thus, proper functioning of all retinae was maintained throughout and was not impaired by the transplantation procedures.

Given the magnification of retinal signals shown by the visual pathway, we reasoned that photoresponses recorded from transplanted *Nrl-GFP*$^+$ rods, although too small in amplitude or too few in number to be detected by ERG, could be transmitted to the brain and generate activity in defined areas of the visual cortex. We therefore performed optical intrinsic imaging[13,14] of primary visual cortex (Fig. 2d, e and Supplementary Fig. 2b). Four overlapping stimuli covering most of the visual field of the stimulated eye were used and consisted of flickering black/white bars on a grey background (Fig. 2e, row i).When presented to wild-type mice ($n = 5$), such stimuli always evoked strong signals in well-defined areas of the visual cortex under both scotopic (Fig.2e, row ii) and photopic (Supplementary Fig. 2b) conditions. Normal retinotopy was observed, as indicated by the different cortical locations of the responses to each stimulus (colour maps; Fig. 2e and Supplementary Fig. 2b). In contrast, no detectable response was observed after scotopic stimulation of untreated *Gnat1*$^{-/-}$ mice ($n = 7$) (Fig. 2e, row iii, and Supplementary Figs 2b and 5). We assessed the impact of transplantation by giving *Gnat1*$^{-/-}$ animals *Nrl-GFP*$^+$ rod precursors or age-matched *Gnat1*$^{-/-}$ (sham) cells, as before. We observed no cortical activity in response to scotopic visual stimuli presented to sham-injected eyes ($n = 3$; Fig. 2e, row iv, and Supplementary Fig. 5), demonstrating that neither injection procedure nor presence of non-functional cells led to false signals in the neocortex. However, presentation of the same stimuli to eyes receiving *Nrl-GFP* transplants led to robust responses in all animals ($n = 5$; Fisher's exact test $P = 0.0175$) (Fig. 2e, row v, and Supplementary Fig. 5); partly overlapping stimuli gave responses in likewise partly overlapping areas of the neocortex, with some preservation of retinotopy in the areas of integration (colour maps; Fig. 2e, row v, and Supplementary Fig. 5). Robust integration (10,782–31,075 cells) was observed in all animals displaying cortical activity. Because transplanted cells

predominantly integrate near the injection site, it is reasonable that only some stimuli led to a reliable cortical response (compare stimuli 1, 3, 4 with stimulus 2, Fig. 2e, row v). Whenever possible, after using scotopic stimuli we assessed photopic stimuli; such stimuli elicited clear responses in all groups.

To address the paramount question of whether photoreceptor transplantation confers improvements in vision, we assessed visual function first by measuring optomotor head-tracking responses to a rotating grating (Fig. 3a, b; see Supplementary Information)[9,15,16]. *Gnat1*$^{-/-}$ mice received dual transplants of *Nrl-GFP*$^{+}$ rod precursors into one eye and age-matched *Gnat1*$^{-/-}$ cells into the contralateral eye, as previously described. Additional cohorts received (1) the same, but using our original protocol[1], (2) dual *Gnat1*$^{-/-}$ sham injections to both eyes or (3) no injection. As expected, no head-tracking behaviour was observed in any *Gnat1*$^{-/-}$ mouse at scotopic luminance levels (Fig. 3c, e) and normal head tracking occurred under photopic conditions (Supplementary Fig. 2c, d) before transplantation. After transplantation, scotopic optomotor responses were only seen in *Nrl-GFP*-treated eyes; mean contrast-sensitivity threshold for *Nrl-GFP*-treated animals was 1.3 ± 0.1 compared with 15.0 ± 0.6 in wild type (Fig. 3c). Murine visual acuity is poorer under scotopic than photopic conditions (0.245 ± 0.01 versus 0.488 ± 0.003 cycles per degree in wild type; see also ref. 9) but a visual-acuity threshold of 0.097 ± 0.007 cycles per degree was recorded in *Nrl-GFP*-treated *Gnat1*$^{-/-}$ mice under the same conditions (Fig. 3e). Moreover, there was a significant positive correlation between both contrast sensitivity (*F*-test, $P < 0.01$; Fig. 3d) and visual acuity (*F*-test, $P < 0.05$; Fig. 3f) and the number of integrated *Nrl-GFP*$^{+}$ rods. Photopic optomotor responses, assessed after scotopic testing, remained unchanged (Fig. 3g, h).

Finally, we assessed vision using the visually guided water-maze test[17], which requires cognitive processing of visual information to associate a grating with escape from a Y-shaped water maze. Under photopic conditions, *Gnat1*$^{-/-}$ mice learned and completed the task as well as wild type (≥70% correct responses; Fig. 4a, Supplementary Fig. 2e–g and Supplementary Information) but performed no better than chance under scotopic conditions. *Gnat1*$^{-/-}$ mice then received (1) dual injections of *Nrl-GFP*$^{+}$ rod precursors to both eyes, (2) sham injections to both eyes or (3) remained untreated. After transplantation, four out of nine *Gnat1*$^{-/-}$ animals receiving *Nrl-GFP*$^{+}$ rod precursors correctly completed the task in at least 70% of trials under scotopic conditions (green bars, Fig. 4b; Supplementary Movie). In contrast, all sham and untreated *Gnat1*$^{-/-}$ mice performed no better than chance (50%). As a group, *Nrl-GFP*-treated animals were significantly better at solving the water-maze task than either control group (Fig. 4c). The four *Nrl-GFP*-treated *Gnat1*$^{-/-}$ animals able to solve the task correctly further had a contrast sensitivity of 1.3 ± 0.04 and visual acuity of 0.09 ± 0.005 cycles per degree (compared with contrast sensitivity of 3.0 ± 0.24 and visual acuity of 0.206 ± 0.005 cycles per degree, respectively, for wild-type controls; Fig. 4d, e). These same animals solved the task with an average swim time of 15.1 ± 0.8 s (correct choice swim-time latency 9.6 ± 0.8 s), compared with 26.4 ± 1.1, 26.0 ± 1.2 and 7.1 ± 1.4 s for sham-injected *Gnat1*$^{-/-}$, untreated *Gnat1*$^{-/-}$ and wild-type mice, respectively (Fig. 4f). There was a significant positive correlation between ability to solve the task and integrated *Nrl-GFP*$^{+}$ rod number (*F*-test, $P < 0.01$; Fig. 4g, h). Cell integration in those animals that performed best in this task was often clustered, rather than widely distributed across the retina, suggesting that proximity of integrated cells to one another may be important, in addition to absolute number. For example, *Nrl-GFP*-treated animals numbers 1 and 2 had similar numbers of integrated rod photoreceptors but number 1 had qualitatively more closely grouped clusters of cells (data not shown). Ability to perform the water-maze task under photopic conditions, assessed after scotopic testing, remained unchanged in all groups after transplantation (Fig. 4i–k).

Although the scotopic visual function recorded here in transplanted *Gnat1*$^{-/-}$ mice is lower than in wild-type animals, such sensitivity is still impressive given that integrated photoreceptors account for less than 1% of the total rods in the retina. However, other studies have demonstrated a remarkable sensitivity from very few light-sensitive cells[18], whereas clinical studies have shown useful vision despite there being no detectable ERG response from the retina[19]. Many additional steps are required before these findings can be translated to the clinic, but the results presented here demonstrate for the first time that transplanted rod-photoreceptor precursors can integrate into a dysfunctional adult retina and, by directly connecting with the host retinal circuitry, truly improve vision.

METHODS SUMMARY

The transplantation procedures were performed as described previously[1,3–5] with modifications, as described in Supplementary Fig. 1 and Supplementary Information. All recipients were adult (6–8 weeks) at time of transplantation and functional assessments were made 4–6 weeks after transplantation. Cellular, retinal and behavioural assessments of visual function were assessed using suction-pipette recordings[12,20], ERGs[21], optical imaging[13,14], optomotor[9,15,16] and watermaze[17] testing and previously published protocols with amendments as detailed in Supplementary Information.

Supplementary Material

Refer to Web version on PubMed Central for supplementary material.

Acknowledgments

This work was supported by the Medical Research Council UK (G03000341), the Wellcome Trust (082217), the Royal Society (RG080398), the British Retinitis Pigmentosa Society (GR566) and The Miller's Trust. R.A.P. is a Royal Society University Research Fellow. R.R.A is partly funded by the Department of Health's National Institute for Health Research Biomedical Research Centre at Moorfields Eye Hospital and Alcon Research Institute. J.C.S. is supported by Great Ormond Street Hospital Children's Charity. T.X. and K.-W.Y. were supported by a US National Institutes of Health grant (EY06837) and the António Champalimaud Vision Award (Portugal). C.H.S. was supported by grants EY11307, EY016805, Research to Prevent Blindness. M.C. holds the GlaxoSmithKline/Fight for Sight Chair in Visual Neuroscience and is supported by the European Research Council. We thank Y. Umino and the late R. Barlow for advice and training with optomotor recordings, A. Eddaoudi for FACS assistance, G. Holder for advice on ERG recordings, C. Hogg for light calibrations, L. Cao for technical suggestions on suction-pipette recordings, and the Department of Genetics, UCL Institute of Ophthalmology, for discussions on the data.

References

1. MacLaren RE, et al. Retinal repair by transplantation of photoreceptor precursors. Nature. 2006; 444:203–207. [PubMed: 17093405]
2. Calvert PD, et al. Phototransduction in transgenic mice after targeted deletion of the rod transducin α-subunit. Proc. Natl Acad. Sci. USA. 2000; 97:13913–13918. [PubMed: 11095744]
3. West EL, et al. Pharmacological disruption of the outer limiting membrane leads to increased retinal integration of transplanted photoreceptor precursors. Exp. Eye Res. 2008; 86:601–611. [PubMed: 18294631]
4. Pearson RA, et al. Targeted disruption of outer limiting membrane junctional proteins (Crb1 and ZO-1) increases integration of transplanted photoreceptor precursors into the adult wild-type and degenerating retina. Cell Transplant. 2010; 19:487–503. [PubMed: 20089206]
5. West EL, et al. Long-term survival of photoreceptors transplanted into the adult murine neural retina requires immune modulation. Stem Cells. 2010; 28:1997–2007. [PubMed: 20857496]
6. Bartsch U, et al. Retinal cells integrate into the outer nuclear layer and differentiate into mature photoreceptors after subretinal transplantation into adult mice. Exp. Eye Res. 2008; 86:691–700. [PubMed: 18329018]

7. Akimoto M, et al. Targeting of GFP to newborn rods by Nrl promoter and temporal expression profiling of flow-sorted photoreceptors. Proc. Natl Acad. Sci. USA. 2006; 103:3890–3895. [PubMed: 16505381]
8. Maeda T, et al. A critical role of CaBP4 in the cone synapse. Invest. Ophthalmol. Vis. Sci. 2005; 46:4320–4327. [PubMed: 16249514]
9. Umino Y, Solessio E, Barlow RB. Speed, spatial, and temporal tuning of rod and cone vision in mouse. J. Neurosci. 2008; 28:189–198. [PubMed: 18171936]
10. Elias RV, et al. Temporal kinetics of the light/dark translocation and compartmentation of arrestin and α-transducin in mouse photoreceptor cells. Mol. Vis. 2004; 10:672–681. [PubMed: 15467522]
11. Garner CC, Kindler S, Gundelfinger ED. Molecular determinants of presynaptic active zones. Curr. Opin. Neurobiol. 2000; 10:321–327. [PubMed: 10851173]
12. Nikonov SS, et al. Physiological features of the S- and M-cone photoreceptors of wild-type mice from single-cell recordings. J. Gen. Physiol. 2006; 127:359–374. [PubMed: 16567464]
13. Grinvald A, et al. Functional architecture of cortex revealed by optical imaging of intrinsic signals. Nature. 1986; 324:361–364. [PubMed: 3785405]
14. Schuett S, Bonhoeffer T, Hubener M. Mapping retinotopic structure in mouse visual cortex with optical imaging. J. Neurosci. 2002; 22:6549–6559. [PubMed: 12151534]
15. Alexander JJ, et al. Restoration of cone vision in a mouse model of achromatopsia. Nature Med. 2007; 13:685–687. [PubMed: 17515894]
16. Prusky GT, et al. Rapid quantification of adult and developing mouse spatial vision using a virtual optomotor system. Invest. Ophthalmol. Vis. Sci. 2004; 45:4611–4616. [PubMed: 15557474]
17. Prusky GT, West PW, Douglas RM. Behavioral assessment of visual acuity in mice and rats. Vision Res. 2000; 40:2201–2209. [PubMed: 10878281]
18. Lagali PS, et al. Light-activated channels targeted to ON bipolar cells restore visual function in retinal degeneration. Nature Neurosci. 2008; 11:667–675. [PubMed: 18432197]
19. Berson EL. Long-term visual prognoses in patients with retinitis pigmentosa: the Ludwig von Sallmann lecture. Exp. Eye Res. 2007; 85:7–14. [PubMed: 17531222]
20. Fu Y, et al. Quantal noise from human red cone pigment. Nature Neurosci. 2008; 11:565–571. [PubMed: 18425122]
21. Tan MH, et al. Gene therapy for retinitis pigmentosa and Leber congenital amaurosis caused by defects in AIPL1: effective rescue of mouse models of partial and complete Aipl1 deficiency using AAV2/2 and AAV2/8 vectors. Hum. Mol. Genet. 2009; 18:2099–2114. [PubMed: 19299492]
22. Wong AA, Brown RE. Age-related changes in visual acuity, learning and memory in C57BL/6J andDBA/2J mice. Neurobiol. Aging. 2007; 28:1577–1593. [PubMed: 17010477]

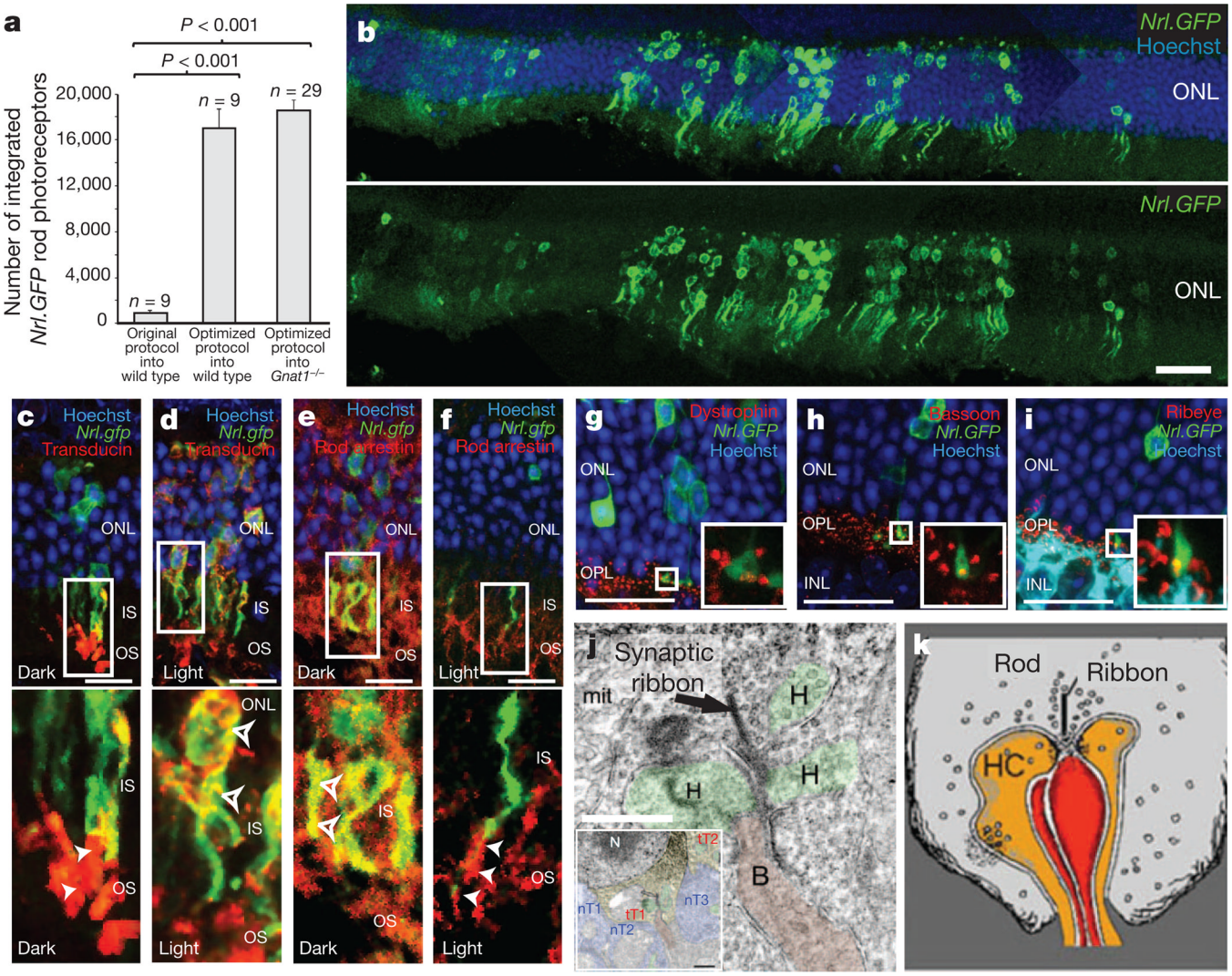

Figure 1. Improved transplantation protocols significantly improve photoreceptor integration into the adult *Gnat1*$^{-/-}$ model of retinal dysfunction

a, *Nrl-GFP*$^{+}$ rod-photoreceptor integration using new and previously published protocols[1]; mean ± s.e.m., analysis of variance (ANOVA); *n*, number of eyes. **b**, Typical example of integrated *Nrl-GFP*$^{+}$ rods (green). Scale bar, 50 μm. **c**–**f**, Integrated *Nrl-GFP*$^{+}$ rods expressed rod-α-transducin (**c**, **d**; red) and rod-arrestin (**e**, **f**; red) and demonstrated correct, counter-directional light-mediated translocation of these proteins (bottom panels in **c**–**f**, respectively). **g**–**i**, Integrated *Nrl-GFP*$^{+}$ rods formed spherule synapses and expressed dystrophin (**g**), bassoon (**h**) and ribeye (**i**) (all red). Inserts, 3 μm projections of regions marked. IS, inner segments; OS, outer segments; ONL, outer nuclear layer; OPL, outer plexiform layer; INL, inner nuclear layer. Scale bar, 10 μm. **j**, Electron micrographs of low- (inset) and high-power views (consecutive sections), showing *Nrl-GFP*$^{+}$ rod terminals (tT1, tT2). tT1 formed classic triad with horizontal axon terminals (H, orange) and bipolar dendritic terminal (B, red). Endogenous rod terminals (nT; blue) were DAB negative. Arrows, synaptic ribbons; scale bars, 500 nm. **k**, Schematic of rod-triad synapse, reproduced with permission from Webvision (H. Kolb *et al.*, http://webvision.med.utah.edu/).

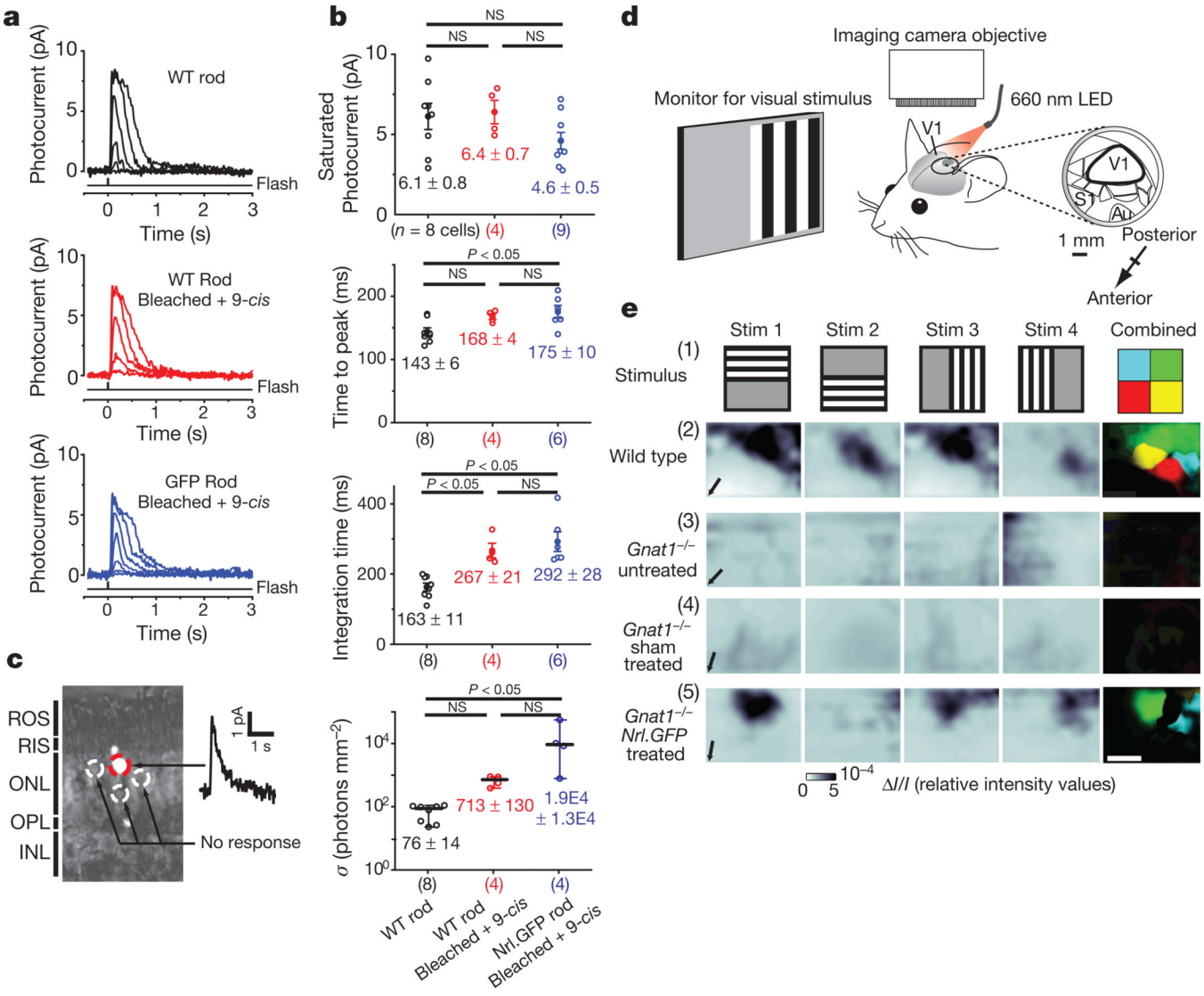

Figure 2. Transplanted *Nrl-GFP*$^{+}$ rod photoreceptors are light-responsive and project light information to the visual cortex

a, Flash-response families from single dark-adapted wild type (black), bleached/regenerated wild type (red) and bleached/regenerated-*Nrl-GFP*$^{+}$ (blue) rods. See Supplementary Information for flash intensities. **b**, Comparison of saturated response amplitude and dim-flash response parameters. Individual data points are shown (open circles) with mean ± s.e.m. (ANOVA, top three panels) or median ± range (Kruskal–Wallis, bottom panel); *n*, number of cells; s, half-saturating flash intensity. Not all parameters were obtainable for each cell. **c**, Representative retinal slice showing light-sensitive *Nrl-GFP*$^{+}$ rod (red circle) and surrounding non-responsive GFP negative rods (white circles). **d**, Schematic of optical intrinsic imaging set-up (see Supplementary Information). Au, auditory cortex; S1, somatosensory cortex. **e**, Visual stimuli (Stim) (1) elicited optical signals in V1 only from *Nrl-GFP*$^{+}$-treated *Gnat1*$^{-/-}$ (5) and wild type (2), but not untreated (3) or sham-injected (4), *Gnat1*$^{-/-}$ eyes. Far right, overlapping parts of the four stimuli were colour-coded (1). Only responses present for two overlapping stimuli were considered genuine sensory-evoked signals and represented with the corresponding colour (2–5). Scale bar, 1 mm.

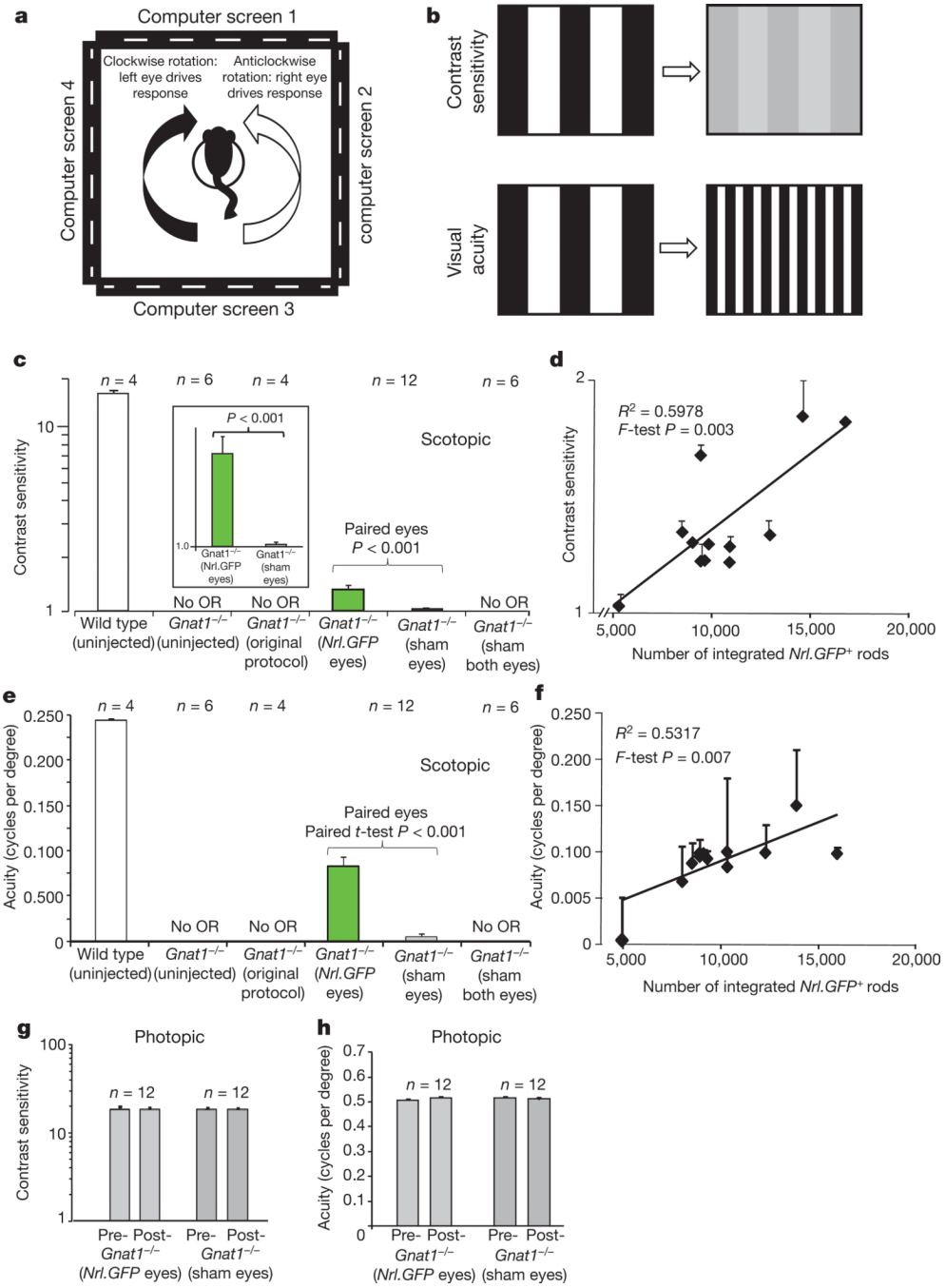

Figure 3. Rescue of scotopic optokinetic head-tracking behaviour in Nrl-GFP-treated *Gnat1*$^{-/-}$ mice

a, The Optomotry™ set-up (see Supplementary Information). **b**, Measures of visual function include contrast sensitivity and visual acuity. **c, d**, Scotopic contrast sensitivity and visual acuity threshold measurements for *Nrl-GFP*-(green bars) or sham-(*Gnat1*$^{-/-}$) treated *Gnat1*$^{-/-}$ eyes, and the averages of left and right eyes for *Gnat1*$^{-/-}$ mice receiving original protocol transplants[1] or sham injections to both eyes, or untreated *Gnat1*$^{-/-}$ or wild type (white bars) controls. OR, optomotor response. Paired *t*-test. **e**, **f**, Scatter plots of contrast sensitivity and visual acuity against integrated *Nrl-GFP*$^{+}$ rod number. **g**, **h**, Photopic contrast

sensitivity and visual acuity for *Nrl-GFP*-(light grey) and sham-treated (dark grey) eyes before and after transplantation. Means ± s.e.m.; *n*, number of animals.

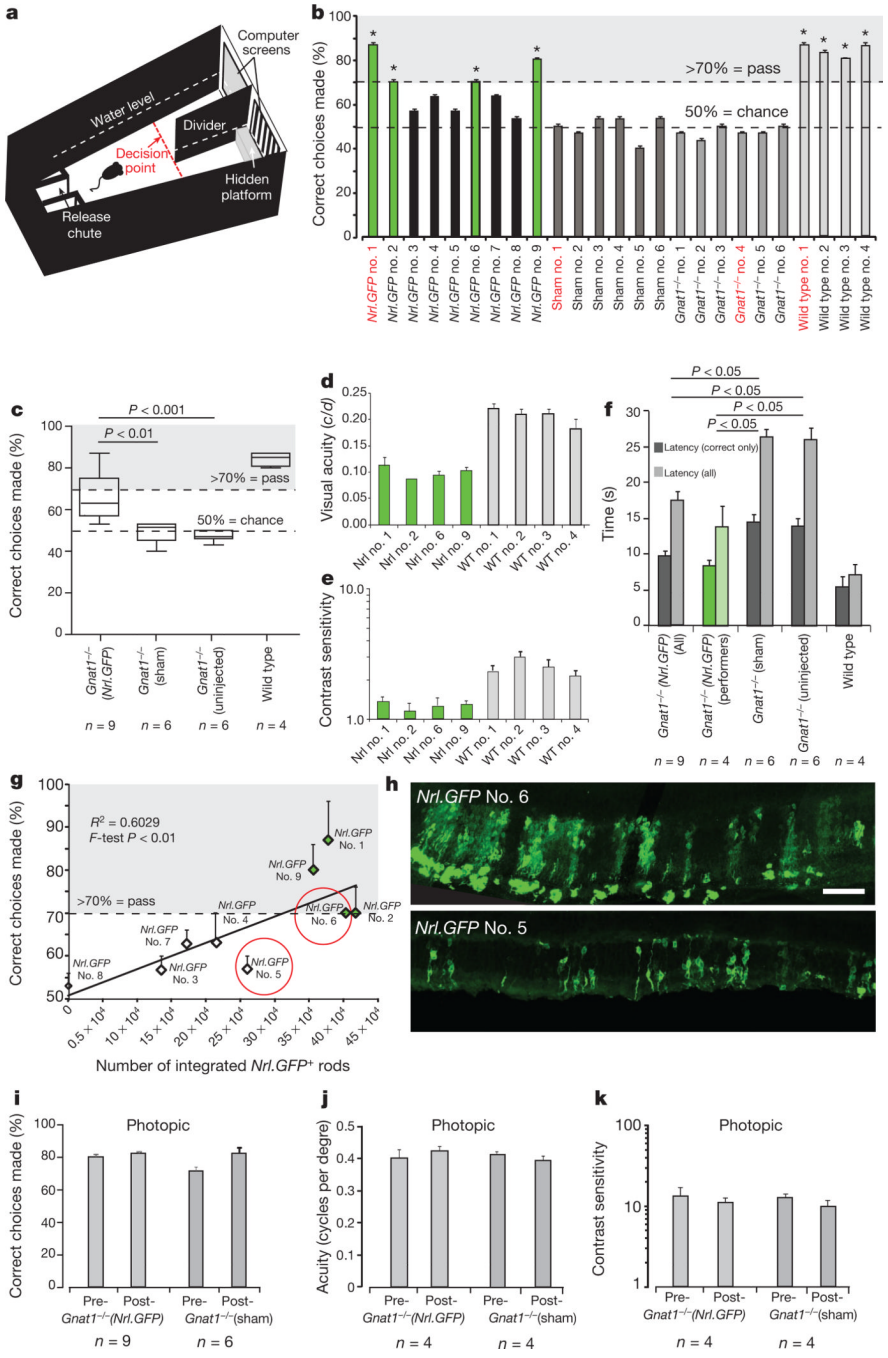

Figure 4. Nrl-GFP-treated *Gnat1*$^{-/-}$ mice can solve the visually guided water-maze task under scotopic conditions

a, Schematic of water-maze apparatus (adapted from ref. 22; see Supplementary Information). Mice were trained to associate striped grating with escape from water by a hidden platform. An animal 'passes' a trial by crossing the red line (decision point) on the side of the divider with the striped grating. **b**, Pass rate of *Nrl-GFP*-treated (black), sham-injected (dark grey) and non-injected (mid grey) *Gnat1*$^{-/-}$ and non-injected wild-type (light grey) mice. *Nrl-GFP*-treated animals with a pass-rate of at least 70% are shown in green throughout. Mouse numbers in red refer to mice shown in Supplementary Movie. **c**, Average performance rate of all groups. **d**, Visual acuity and **e**, contrast sensitivity measurements for

responders from *Nrl-GFP*-treated (green) and wild-type (light grey) groups. **f**, Swim-time latencies (time-to-platform) for all (light grey) and correct choice-only (dark grey) trials. **g**, Ability to solve water-maze task plotted against integrated *Nrl-GFP* photoreceptor number. **h**, Examples of integration in animals that successfully (top; *Nrl-GFP*-treated, number 6) or unsuccessfully (bottom; *Nrl-GFP*-treated, number 5) solved the task, as indicated in **g** (circled, red). Scale bar, 100 μm. **i**–**k**, Pass rate (**i**), visual acuity (**j**) and contrast sensitivity (**k**) for *Nrl-GFP*-treated (light grey bars) and sham-injected (dark grey bars) *Gnat1*$^{-/-}$ mice before and after transplantation under photopic conditions. Means ± s.e.m.; ANOVA; *n*, number of animals.